

# Asteroseismic imprints of strong non-axisymmetric fields in the cores of red giants

Nicholas Z. Rui,<sup>1,2,3</sup> J. M. Joel Ong,<sup>4</sup> Armand Leclerc,<sup>5</sup> Daniel Lecoanet,<sup>2,6</sup> Lisa Bugnet,<sup>5</sup> Janosz W. Dewberry,<sup>7</sup> Bastien Liagre,<sup>8</sup> and Stéphane Mathis<sup>9</sup>

<sup>1</sup>Department of Astrophysical Sciences, Princeton University, 4 Ivy Lane, Princeton, NJ 08544, USA

<sup>2</sup>Center for Interdisciplinary Exploration and Research in Astrophysics (CIERA), Northwestern University, 1800 Sherman Ave., Evanston, IL 60201, USA

<sup>3</sup>NASA Hubble Fellow

<sup>4</sup>Sydney Institute for Astronomy, University of Sydney, A28 Physics Road, Sydney NSW 2006, Australia

<sup>5</sup>Institute of Science and Technology Austria, Am Campus 1, Klosterneuburg, 3400, Austria

<sup>6</sup>Department of Engineering Sciences and Applied Mathematics, McCormick School of Engineering, Northwestern University, 2145 Sheridan Road, Evanston, IL 60208, USA

<sup>7</sup>Department of Astronomy, University of Massachusetts Amherst, 710 N Pleasant St, Amherst, MA 01003, USA

<sup>8</sup>Université Paris Cité, Université Paris-Saclay, CEA, CNRS, AIM, F-91191 Gif-sur-Yvette, France

<sup>9</sup>Université Paris-Saclay, Université Paris Cité, CEA, CNRS, AIM, F-91191 Gif-sur-Yvette, France

---

## Abstract

To date, magnetic fields have been asteroseismically measured in nearly one hundred red giant cores. However, most analyses assume weak magnetic fields and slow rotation so that perturbation theory can be applied. The “traditional approximation of rotation and magnetism” (TARM) method can predict gravity-mode frequencies under strong magnetic fields and rapid rotation rates. So far, this formalism requires the magnetic field to be symmetric about the rotation axis.

We generalize the TARM formalism to apply to arbitrary magnetic field geometries, including cases where the magnetic and rotation axes are misaligned, as well as fields with no symmetry axis at all. The resulting gravity modes exhibit a rich diversity of wave behavior, including oblique pulsation and avoided crossings. We also clarify the domains of validity of perturbation theory and the TARM formalism.

---

## 1 Introduction

Asteroseismology has very recently offered the only direct glimpses into magnetic fields in the deep interiors of stars. The Lorentz forces associated with these magnetic structures increase the frequencies of gravity (g) modes in a distinctive way (e.g., Mathis *et al.*, 2021; Bugnet *et al.*, 2021) which has to date been used to infer strong near-core magnetic fields in roughly 80 red giants (Li *et al.*, 2022; Deheuvels *et al.*, 2023; Li *et al.*, 2023; Hatt *et al.*, 2024; Villate *et al.*, 2026; Deheuvels *et al.*, 2026) as well as in a handful of main-sequence stars (Vandersnickt *et al.*, 2025; Takata *et al.*, 2026; Ihallaine *et al.*, 2026). Approximately one-fifth of red giants also exhibit suppressed dipole modes (Stello *et al.*, 2016) which are usually attributed to magnetic suppression Fuller *et al.* (2015) by strong magnetic fields. Magnetic suppression of g modes is expected to occur when the field strength exceeds a frequency-dependent threshold given by Fuller *et al.* (2015):

$$B_{r,\text{crit}} \sim \sqrt{\rho} \omega^2 r / N, \quad (1)$$

where  $\rho$  is the density,  $\omega$  is the mode frequency,  $r$  is the radial coordinate, and  $N$  is the Brunt–Väisälä frequency. At these field strengths (typically  $\approx 10^5$ – $10^6$  G in red giant cores), magnetic forces become comparable to buoyant ones and are expected to affect efficient dissipation of g-mode energy, although the exact mechanism is not well understood (Loi &

Papaloizou, 2017; Loi, 2020; Lecoanet *et al.*, 2017, 2022; Rui & Fuller, 2023; Müller *et al.*, 2025; David *et al.*, 2025).

Most asteroseismic observations of magnetically induced frequency shifts are interpreted using perturbation theory, which assumes that magnetic fields are weak (e.g., Gough & Thompson, 1990). In particular, perturbation theory ignores the ability of strong magnetic fields to significantly deform the structures of g modes themselves, an assumption which fails when the Lorentz force is comparable to buoyancy. This hypothesis breaks down for stars with “near-critical” magnetic fields which are too strong for perturbation theory to be valid but not so strong that magnetic suppression is expected to make oscillation modes unmeasurable.

Rui & Fuller (2023) and Rui *et al.* (2024) recently developed a non-perturbative formalism for predicting frequency shifts due to near-critical magnetic fields based on the *traditional approximation of rotation and magnetism* (TARM). This formalism takes advantage of the short radial wavelengths  $\lambda_r = 2\pi/k_r$  of g modes in red giants and many main-sequence stars, which follows from the gravity-wave dispersion relation  $k_r \approx \sqrt{\ell(\ell+1)}N/\omega r$  where  $N/\omega \gg 1$  ( $\approx 100$  for typically excited modes in red giant cores). This property allows the perturbed magnetohydrodynamic equations to be approximately separated in the radial and horizontal directions. This is akin to the standard mathematical treatment

for waveguides (e.g., Jackson & Fox, 1999). It is also directly analogous to the calculation of g-mode frequencies affected by strong Coriolis forces under the *traditional approximation of rotation* (TAR; e.g., Hough, 1897, 1898; Bildsten *et al.*, 1996; Lee & Saio, 1997). A prerequisite for applying the TARM formalism is that the magnetic field be axisymmetric about the rotation axis.

Deheuvels *et al.* (2026) recently applied the TARM formalism to the fitting of 8 red giants possessing near-critical core magnetic fields. The detection of non-perturbative frequency shifts allows some constraint on the radial structure of the field, which Deheuvels *et al.* (2026) find to be roughly confined to layers which previously belonged to the main-sequence convective core (suggestive of a dynamo origin for the field; Cantiello *et al.*, 2016). However, our ability to probe the full diversity of magnetic structures in stellar interiors is inhibited by our inability to predict g-mode frequencies under strong, non-axisymmetric magnetic fields. This Proceeding summarizes our recent progress in extending the TARM formalism to non-axisymmetric magnetorotational structures, with more details given in a recently submitted manuscript (Rui *et al.*, 2026).

## 2 Formalism and Results

The propagation of magnetogravity waves is governed by the linearized magneto-Boussinesq equations (Proctor & Weiss, 1982; Lecoanet *et al.*, 2017):

$$\begin{aligned} \rho_0 \partial_t^2 \vec{\xi} + 2\rho_0 \vec{\Omega} \times \partial_t \vec{\xi} \\ = -\nabla \left( p' + \frac{1}{4\pi} \vec{B}_0 \cdot \vec{B}' \right) - \rho_0 N^2 \xi_r \hat{r} + \frac{1}{4\pi} \left( \vec{B}_0 \cdot \nabla \right) \vec{B}' \end{aligned} \quad (2a)$$

$$\nabla \cdot \vec{\xi} = 0, \quad (2b)$$

where  $p'$ ,  $\vec{\xi}$ , and  $\vec{B}'$  are the pressure, fluid displacement, and magnetic field perturbations,  $\vec{\Omega} = \Omega \hat{z}$  is the rotation vector (rigid rotation has been assumed), and subscripts “0” indicate equilibrium quantities.

The content of the TARM is to approximate both  $\vec{\Omega}$  and  $\vec{B}_0$  as being purely radial:

$$\vec{\Omega} \simeq \Omega \cos \theta \hat{r} \quad (3a)$$

$$\vec{B}_0 \simeq B_{0r}(r) \psi(\theta, \phi; r) \hat{r}, \quad (3b)$$

where we hereafter suppress the radial argument in  $\psi$ . The TARM is justified for small radial wavelengths  $\lambda_r$ , as long as the horizontal component of  $\vec{B}_0$  is not stronger than the radial component by a large factor  $\sim \lambda_h/\lambda_r$ . For standing magnetogravity modes for which perturbations have a sinusoidal time dependence  $\propto e^{i\omega t}$ , we make the following Jefferys–Wentzel–Kramers–Brillouin (JWKB) ansatz:

$$p' = \rho_0 \omega^2 r^2 \sum_{\alpha} A_{\alpha}(r) \pi_{\alpha}(\theta, \phi; r) e^{-iS_{\alpha}(r)/\epsilon} \quad (4a)$$

$$\vec{\xi}_h = r \sum_{\alpha} A_{\alpha}(r) \vec{\zeta}_{\alpha}(\theta, \phi; r) e^{-iS_{\alpha}(r)/\epsilon}, \quad (4b)$$

where the JWKB actions  $S_{\alpha}$  are related to  $k_r$  as  $k_r = S'_{\alpha}/\epsilon$ . The dimensionless perturbations  $(\pi_{\alpha}, \vec{\zeta}_{\alpha})$  are defined to in-

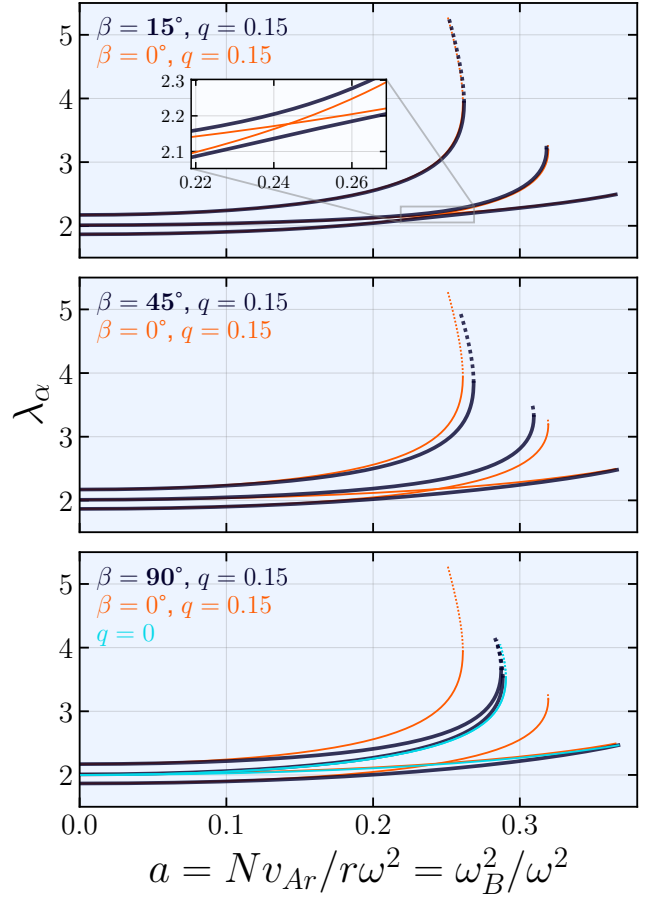


Figure 1: Eigenvalues  $\lambda_{\alpha}$  for dipole magnetogravity polarizations under an inclined dipolar magnetic field (Equation 7). Reproduced from Figure 5 of Rui *et al.* (2026).

dividually satisfy Equations 2 to lowest-order in  $\epsilon$ :

$$(1 - b_{\alpha}^2 \psi^2) \vec{\zeta}_{\alpha} - i q \mu \hat{r} \times \vec{\zeta}_{\alpha} - \vec{\nabla}_h \pi_{\alpha} = 0 \quad (5a)$$

$$\lambda_{\alpha} \pi_{\alpha} + \vec{\nabla}_h \cdot \vec{\zeta}_{\alpha} = 0, \quad (5b)$$

where  $q = 2\Omega/\omega$  and  $b_{\alpha} = k_{r,\alpha} v_{Ar}/\omega$ . The index  $\alpha$  labels families of solutions to the eigenvalue problem in Equations 5, hereafter referred to as “magnetogravity polarizations” in analogy to waves with transverse degrees of freedom. We solve Equations 5 as a function of  $q$  and  $b_{\alpha}$  using the spectral eigenvalue solver of *Dedalus* (Burns *et al.*, 2020). For practical purposes, we reparameterize the dimensionless magnetic field strength in terms of

$$a = \frac{b_{\alpha}}{\sqrt{\lambda_{\alpha}}} = \left( \frac{N}{\omega} \right) \left( \frac{v_{Ar}/r}{\omega} \right). \quad (6)$$

The utility of this choice is described in detail in Section 3.2 of Rui *et al.* (2024).

We first consider the simple case of a dipolar magnetic field inclined from the rotation axis by a misalignment angle  $\beta$ :

$$\psi(\theta, \phi) = \sqrt{3} (\cos \beta \cos \theta + \sin \beta \sin \theta \cos \phi). \quad (7)$$

Figure 1 shows the eigenvalues  $\lambda_{\alpha}$  for the dipole ( $\ell = 1$ )

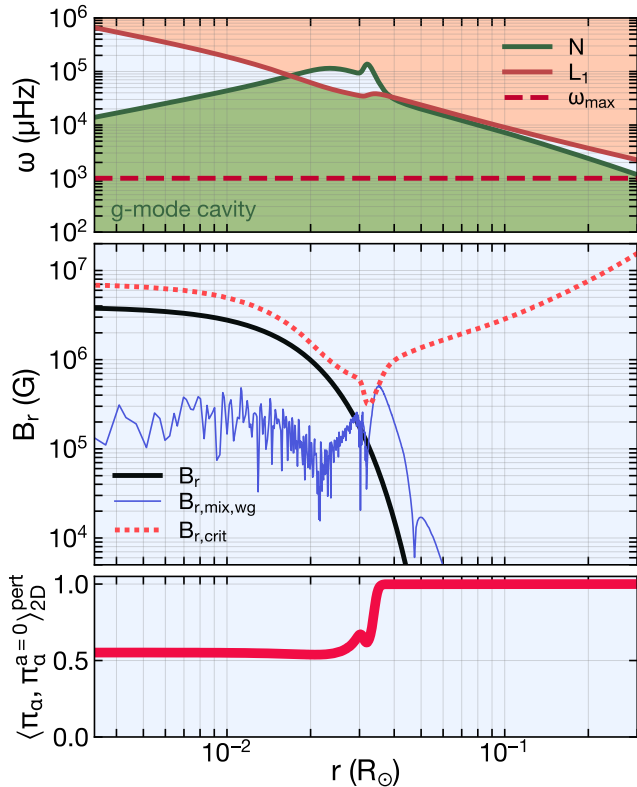


Figure 2: *Top*: Asteroseismic propagation diagram for a  $1.2M_{\odot}$ ,  $5R_{\odot}$  red giant MESA model. *Middle*:  $B_{r,\text{mix,wg}}$  (Equation 8) given a prescribed background magnetic field profile (black), compared to  $B_{r,\text{crit}}$  (Equation 1). *Bottom*: Assuming an inclined dipolar magnetic field with  $\beta = 90^\circ$ , the degree to which a magnetogravity polarization’s horizontal structure differs from its structure at  $a = 0$ . Reproduced from Figure 11 of Rui *et al.* (2026).

magnetogravity polarizations for magnetic fields with different values of  $\beta$ . For small misalignments, the eigenvalues  $\lambda_{\alpha}$  are very similar to their values in the aligned case ( $\beta = 0^\circ$ ; orange curves in Figure 1). However, unlike in the aligned case, the eigenvalues of the  $m = -1$  and  $m = 0$  magnetogravity polarizations are prevented from crossing by an avoided crossing (shown in the inset in the top panel of Figure 1). At this avoided crossing, the two magnetogravity polarizations rapidly exchange character, varying significantly in horizontal structure in the process. As the misalignment  $\beta$  is increased, the avoided crossing broadens until the magnetogravity polarizations are well-separated in  $\lambda_{\alpha}$ .

Rui & Fuller (2023) and Rui *et al.* (2024) assumed that magnetogravity waves perfectly follow a single polarization branch as they propagate in radius (the “adiabatic” assumption in JWKB theory). However, retention of higher-order JWKB terms reveals that magnetogravity waves can convert polarizations as they propagate. Heuristically, “polarization mixing” occurs when the eigenvalues  $\lambda_{\alpha}$  are close together and the change in the structure of one polarization geometrically overlaps with the structure of another polarization. Polarization mixing occurs when the magnitude of the radial

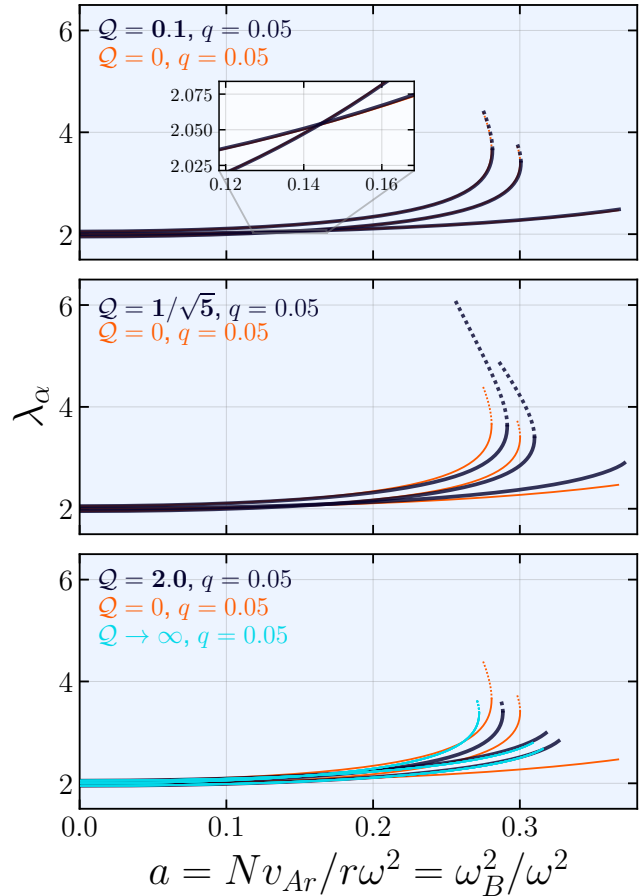


Figure 3: Same as Figure 1 but for a non-axisymmetric dipole-plus-quadrupole geometry (Equation 9). Reproduced from Figure 8 of Rui *et al.* (2026).

component of the magnetic field  $B_r$  locally drops below

$$B_{r,\text{mix,wg}} \simeq \frac{4}{[\ell(\ell+1)]^{1/4}} \left(\frac{\omega}{N}\right)^{1/2} \left(\frac{r}{H_{\alpha\beta}}\right)^{1/2} B_{r,\text{crit}}, \quad (8)$$

where  $H_{\alpha\beta}$  is the radial scale over which two polarizations  $\alpha$  and  $\beta$  “rotate into each other” as they propagate. Figure 2 shows this quantity for a stellar model of a  $1.2M_{\odot}$ ,  $5R_{\odot}$  red giant created using Modules for Experiments in Stellar Astrophysics (MESA; Paxton *et al.*, 2011, 2013, 2015, 2018, 2019; Jermyn *et al.*, 2023). Due to the rapid variation in background quantities near the hydrogen burning shell, we find that this polarization mixing is generically expected to occur unless it is geometrically forbidden for symmetry reasons. The criterion in Equation 8 is related to the breakdown condition for perturbation due to magnetic mixing between modes of different radial orders. Near-degeneracy effects associated with this coupling between radial orders will be the subject of a forthcoming study (Liagre *et al.*, in preparation).

However, single-polarization propagation is still approximately expected when symmetry concerns forbid polarization mixing. The phenomenon of polarization mixing went unnoticed in previous studies (e.g., Lecoanet *et al.*, 2017; Rui & Fuller, 2023; Rui *et al.*, 2024) precisely because the axisym-

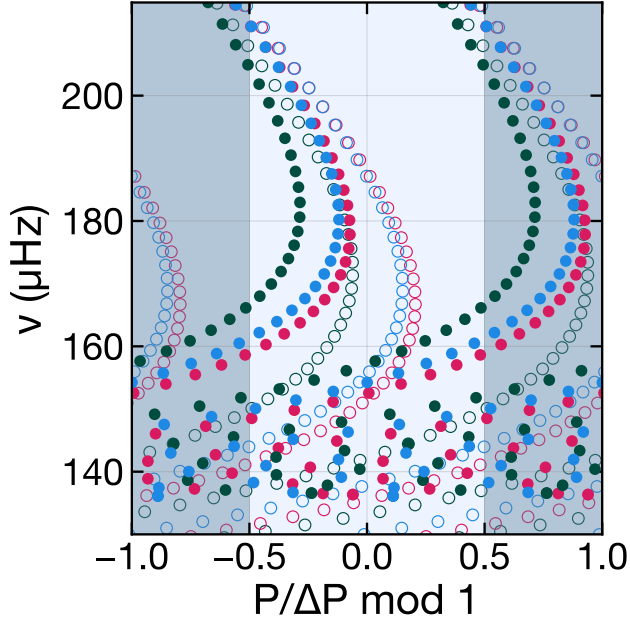


Figure 4: Mock echelle diagram for red-giant dipole g modes which have been strongly perturbed by a non-axisymmetric dipole-plus-quadrupole magnetic field. Open circles indicate the predictions of perturbation theory (e.g., Li *et al.*, 2022). Adapted from Figure 10 of Rui *et al.* (2026).

metry of the field geometries they studied prevented mixing between polarizations with differing azimuthal quantum number  $m$ . However, discrete symmetries can also enforce single-polarization propagation. We illustratively consider the following field geometry:

$$\psi(\theta, \phi) = \frac{1}{\sqrt{1+Q^2}} \left( \sqrt{3} \cos \theta + Q \sqrt{15/4} \sin^2 \theta \cos(2\phi) \right), \quad (9)$$

which is the sum of a real  $m = 0$  dipole and  $m = 2$  quadrupole spherical harmonic, with relative weighting given by  $Q$ . Figure 3 shows the eigenvalues  $\lambda_\alpha$  for this non-axisymmetric dipole-plus-quadrupole geometry for different values of  $Q$ . Unlike in the inclined dipole case, the eigenvalues of dipole polarizations under this geometry are allowed to cross. This is due to the discrete symmetries present in Equation 9, which prohibit mixing between  $\ell = 1$  polarizations in spite of the lack of any continuous rotational symmetry. Under single-polarization propagation, we can straightforwardly calculate predicted mode frequencies by implicitly solving

$$\pi(n + \epsilon_g) = \int_{\mathcal{R}} \frac{\sqrt{\lambda_\alpha(a, q)} N}{\omega r'} dr' \quad (10)$$

for  $\omega$ , where  $\mathcal{R}$  denotes the g-mode cavity (note the  $\omega$  dependence within  $a$  and  $q$ ). Figure 4 presents a mock echelle diagram for our red giant stellar model. As in Rui *et al.* (2024) for axisymmetric field geometries, we find that perturbation theory underestimates frequency shifts due to near-critical magnetic fields.

### 3 Outlook

The near-critical magnetic red giants discovered by Deheuvels *et al.* (2026) are well-fit by axisymmetric magnetic fields embedded deeply within essentially non-rotating cores. Are these near-critical magnetic red giants representative of a distinct subclass of red giants? Should we read deeply into their unusually slowly rotating cores, for example in claiming to better understand magnetic angular momentum transport processes (Fuller *et al.*, 2019; Skoutnev & Beloborodov, 2025)? Unfortunately, due to deep selection biases within the current sample of magnetic red giants, the answers to these questions remain elusive. Theoretical limitations presently prevent us from *discovering* near-critical magnetic red giants whose magnetorotational configurations are outside of a small, especially symmetric subset of all possible geometries. A more general theory of g-mode asteroseismology under strong magnetic fields will require confronting the complex phenomenology associated with polarization mixing. This way lies a more complete understanding of the full diversity of magnetorotational structures in stellar interiors.

### Acknowledgments

N.Z.R. acknowledges support from the NASA Hubble Fellowship grant HST-HF2-51589.001-A awarded by the Space Telescope Science Institute, which is operated by the Association of Universities for Research in Astronomy, Inc., for NASA, under contract NAS5-26555. J.M.J.O. acknowledges support from the Australian Research Council (ARC) through grants DP210103119 and FL220100117. L.B. and A.L. gratefully acknowledge support from the European Research Council (ERC) under the Horizon Europe programme (Calcifer; Starting Grant agreement N°101165631). D.L. is partially supported by NSF AAG grant AST-2405812, Sloan Foundation grant FG-2024-21548 and Simons Foundation grant SFI-MPS-T-MPS-00007353. S.M. acknowledges support from the European Research Council (ERC) under the Horizon Europe programme (Synergy Grant agreement 101071505: 4D-STAR), from the CNES SOHO-GOLF and PLATO grants at CEA-Dap, and from PNPS (CNRS/INSU). While partially funded by the European Union, views and opinions expressed are, however, those of the authors only and do not necessarily reflect those of the European Union or the European Research Council. Neither the European Union nor the granting authority can be held responsible for them.

### References

- Bildsten, L., Ushomirsky, G., & Cutler, C. 1996, *ApJ*, 460, 827.
- Bugnet, L., Prat, V., Mathis, S., Astoul, A., Augustson, K., *et al.* 2021, *A&A*, 650, A53.
- Burns, K. J., Vasil, G. M., Oishi, J. S., Lecoanet, D., & Brown, B. P. 2020, *Physical Review Research*, 2, 023068.
- Cantiello, M., Fuller, J., & Bildsten, L. 2016, *ApJ*, 824, 14.
- David, C. S., Lecoanet, D., & Garaud, P. 2025, *arXiv e-prints*, arXiv:2510.14026.
- Deheuvels, S., Ballot, J., Lignières, F., Li, G., & Villate, M. 2026, *arXiv e-prints*, arXiv:2604.09901.
- Deheuvels, S., Li, G., Ballot, J., & Lignières, F. 2023, *A&A*, 670, L16.
- Fuller, J., Cantiello, M., Stello, D., Garcia, R. A., & Bildsten, L. 2015, *Science*, 350, 423.

- Fuller, J., Piro, A. L., & Jermyn, A. S. 2019, MNRAS, 485, 3661.
- Gough, D. O. & Thompson, M. J. 1990, MNRAS, 242, 25.
- Hatt, E. J., Ong, J. M. J., Nielsen, M. B., Chaplin, W. J., Davies, G. R., *et al.* 2024, MNRAS, 534, 1060.
- Hough, S. S. 1897, Philosophical Transactions of the Royal Society of London Series A, 189, 201.
- Hough, S. S. 1898, Philosophical Transactions of the Royal Society of London Series A, 191, 139.
- Ihallaine, S., Ballot, J., Lignières, F., Ferrié, L., Charpinet, S., *et al.* 2026, *Seismic signature of a magnetic field in the  $\gamma$  Doradus star KIC 2309579*.
- Jackson, J. D. & Fox, R. F. 1999, American Journal of Physics, 67, 841.
- Jermyn, A. S., Bauer, E. B., Schwab, J., Farmer, R., Ball, W. H., *et al.* 2023, ApJS, 265, 15.
- Lecoanet, D., Bowman, D. M., & Van Reeth, T. 2022, MNRAS, 512, L16.
- Lecoanet, D., Vasil, G. M., Fuller, J., Cantiello, M., & Burns, K. J. 2017, MNRAS, 466, 2181.
- Lee, U. & Saio, H. 1997, ApJ, 491, 839.
- Li, G., Deheuvels, S., Ballot, J., & Lignières, F. 2022, Nature, 610, 43.
- Li, G., Deheuvels, S., Li, T., Ballot, J., & Lignières, F. 2023, A&A, 680, A26.
- Loi, S. T. 2020, MNRAS, 493, 5726.
- Loi, S. T. & Papaloizou, J. C. B. 2017, MNRAS, 467, 3212.
- Mathis, S., Bugnet, L., Prat, V., Augustson, K., Mathur, S., *et al.* 2021, A&A, 647, A122.
- Müller, J., Coppée, Q., & Hekker, S. 2025, A&A, 696, A134.
- Paxton, B., Bildsten, L., Dotter, A., Herwig, F., Lesaffre, P., *et al.* 2011, ApJS, 192, 3.
- Paxton, B., Cantiello, M., Arras, P., Bildsten, L., Brown, E. F., *et al.* 2013, ApJS, 208, 4.
- Paxton, B., Marchant, P., Schwab, J., Bauer, E. B., Bildsten, L., *et al.* 2015, ApJS, 220, 15.
- Paxton, B., Schwab, J., Bauer, E. B., Bildsten, L., Blinnikov, S., *et al.* 2018, ApJS, 234, 34.
- Paxton, B., Smolec, R., Schwab, J., Gautschy, A., Bildsten, L., *et al.* 2019, ApJS, 243, 10.
- Proctor, M. R. E. & Weiss, N. O. 1982, Reports on Progress in Physics, 45, 1317.
- Rui, N. Z. & Fuller, J. 2023, MNRAS, 523, 582.
- Rui, N. Z., Ong, J. M. J., Leclerc, A., Lecoanet, D., Bugnet, L., *et al.* 2026, arXiv e-prints, arXiv:2606.07787.
- Rui, N. Z., Ong, J. M. J., & Mathis, S. 2024, MNRAS, 527, 6346.
- Skoutnev, V. A. & Beloborodov, A. M. 2025, ApJL, 989, L4.
- Stello, D., Cantiello, M., Fuller, J., Huber, D., García, R. A., *et al.* 2016, Nature, 529, 364.
- Takata, M., Murphy, S. J., Kurtz, D. W., Saio, H., & Shibahashi, H. 2026, MNRAS, 545, staf2153.
- Vandersnickt, J., Vanlaer, V., Vanrespaille, M., & Aerts, C. 2025, A&A, 704, L13.
- Villate, M., Deheuvels, S., & Ballot, J. 2026, arXiv e-prints, arXiv:2602.14570.